Cellulose (2019) 26:6087–6098
https://doi.org/10.1007/s10570-019-02495-w

ORIGINAL RESEARCH

Facile preparation of high dielectric flexible films based on titanium dioxide and cellulose nanofibrils

Jie Tao · Shun-an Cao · Wei Liu · Yulin Deng

Received: 16 January 2019 / Accepted: 8 May 2019 / Published online: 18 May 2019
© Springer Nature B.V. 2019

Abstract A series of high dielectric composite films based on low-cost and eco-friendly titanium dioxide (TiO_2) and cellulose nanofibril (CNF) was prepared under a facile condition. The relative dielectric constants (ε_r) and dielectric loss ($\tan\delta$) were studied as the function of frequency and filler content. The ε_r of CNF/TiO_2 composite film was 19.51 (at 1 kHz) with a relatively low dielectric loss. Compared with pure CNF films (ε_r = 6.92 at 1 kHz), the ε_r of the composite film was improved about three times with the dielectric loss increased slightly. The effects of TiO_2 addition and hot-press treatment on microstructure, thermal stability, and dynamic mechanical properties of the composite films were also analyzed. It was found that the addition of TiO_2 particles reduces the cellulose–cellulose bonding so generates more pores in the films, which has significant impacts on both dielectric and physical strength properties.

J. Tao · S. Cao (✉)
School of Power and Mechanical Engineering, Wuhan University, Wuhan 430072, Hubei, China
e-mail: 13807138268@163.com

W. Liu · Y. Deng (✉)
School of Chemical and Biomolecular Engineering and Renewable Bioproducts Institute, Georgia Institute of Technology, Atlanta, GA 30332-0620, USA
e-mail: yulin.deng@rbi.gatech.edu

Graphical abstract

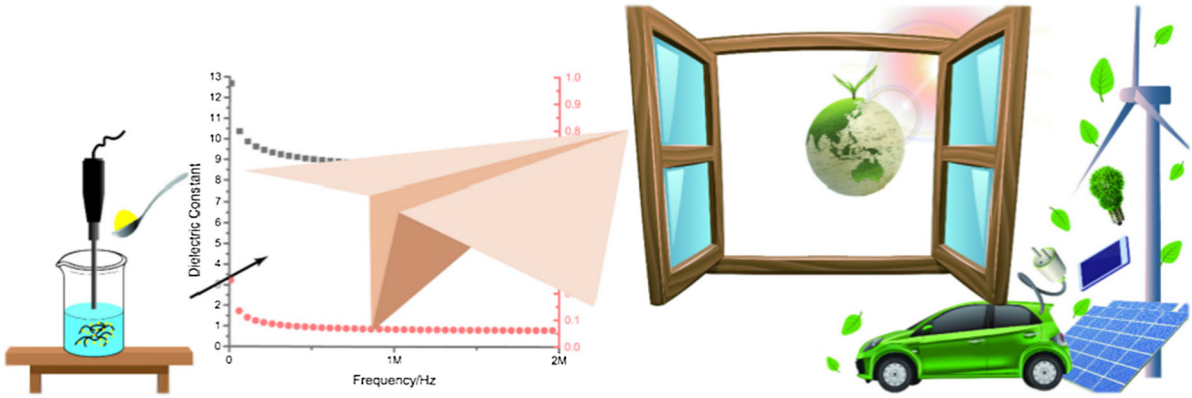

Keywords Film capacitor · Cellulose nanofibril · High dielectric · Titanium dioxide

Introduction

With the fast-growing of advanced electronics and electric power system, soft film capacitors with both high-power and high-energy density at the same time have drawn more and more attention (Dang 2018). This film capacitors (TFCs) usually request high capacity density, large breakdown strength [typically exceeds 300 MV m^{-1} (Paniagua et al. 2014)], high-frequency response, fast charge/discharge speed, low dissipation, and long lifetime. Compared with electrochemical capacitors and batteries, the charge/discharge speed of capacitors depends on their polarizations, which are contributed by the orientation of dipoles and deformations of atoms and molecules and are much faster and less influenced by high frequency than charge carriers transport. With higher dielectrics, the capacitors with same capacitance can be smaller in size and lighter in weight, thus have higher capacity density. Polymer-based dielectrics surpass ceramics by its higher breakdown strength, lower dissipation, easier preparation and longer lifetime.

The most commonly used dielectric polymers for TFCs mainly are non-biodegradable and nonrenewable thermoplastic polymers, such as polypropylene (PP) (Kumari and Ghosh 2018; Lay et al. 2018), polyethylene terephthalate (PET) (Tang et al. 2018; Topala et al. 2007), polyethylene naphthalate (PEN), polyphenylene sulfide (PPS), polytetrafluoroethylene (PTFE) (Thomas et al. 2008; Wang and Dang 2018; Yuan et al. 2014, 2018) and polystyrene (PS). Besides, other polymers include polyimide (PI) (Chang et al. 2009; Feng et al. 2013, 2014; Ishmael et al. 2014; Kizilkaya et al. 2012; Koytepe et al. 2008; Lay et al. 2018; Lee et al. 2009, 2012; Lee and Wang 2010; Lin et al. 2017; Lu et al. 2017; Meena et al. 2012; Olariu et al. 2017; Wang et al. 2018, 2010b; Wu et al. 2017; Yin et al. 2014; Zha et al. 2010a, b), polyamide (PA) (Novac et al. 2017; Qi et al. 2017, 2018), and polyvinylidene fluoride (PVDF) (Al-Saygh et al. 2017; Alam et al. 2017; Deshmukh et al. 2017; Dou et al. 2017; Gan and Abd Majid 2014; Park et al. 2013; Prabakaran et al. 2014; Rekik et al. 2013; Ribeiro et al. 2018; Su et al. 2016; Wang et al. 2010b; Yang et al. 2016) are also studied. PI-based nanocomposites are reported to have enhanced corona aging performance (Lin et al. 2017; Lu et al. 2017; Yin et al. 2014; Zha et al. 2010a), but their relative dielectric constant is generally below 6 (1 kHz) (Feng et al. 2013, 2014; Lay et al. 2018; Wang et al. 2018). Qi et al. prepared polyamide11 (PA11)/$BaTiO_3$/carbon nanotube (CNT) ternary nanocomposites with 3D segregated percolation routes, the relative dielectric constant is 16.2 with a dielectric loss of $\sim$ 0.08 (1 kHz) (Qi et al. 2018). Alam et al. (2017) put titanium dioxide (TiO_2) nanoparticles into γ-phase containing PVDF, and the dielectric constant of the nanocomposite film reaches 32 with a dielectric loss of 0.25 (1 kHz). Recently, low-cost and eco-friendly cellulose nanofibrils are being increasingly explored as a candidate to replace some conventional dielectric materials (Abdel-karim et al. 2018; Al-Saygh et al. 2017; Bonardd et al. 2018; Chiang and Popielarz 2002; Gaspar et al. 2014; Inui

et al. 2015; Jayaramudu et al. 2018b; Le Bras et al. 2015; Madusanka et al. 2016, 2017; Milinskii et al. 2018; Milovidova et al. 2014; Poyraz 2018; Poyraz et al. 2017b; Rajala et al. 2016; Shi et al. 2018; Yagyu et al. 2017; Zeng et al. 2016; Zhou et al. 2018).

Cellulose nanofibril (CNF) has a low density and coefficient of thermal expansion (CTE) (12–28.5 ppm K^{-1}), high mechanical strength (200–400 MPa) and Young's modulus (7.4–14 GPa), excellent thermal stability (> 180 °C) and chemical durability, and it is an almost inexhaustible green material (Du et al. 2017; Fujisaki et al. 2014). The relative dielectric constant (ε_r) of traditional paper prepared from micro-sized cellulose is in the low range of 1.3–4.0, resulting from the porous microstructure (Inui et al. 2014; Inui et al. 2015). With a densely packed nanostructure, the ε_r of nanocellulose paper reaches 5.3 (at 1.1 GHz) (Inui et al. 2014, 2015) with a breakdown strength of 613.8 kV cm^{-1} (Zeng et al. 2016), making it a promising candidate for the dielectric matrix. Comparing to regenerated cellulose films that usually need toxic and expensive solvent, nanocelluloses can be made from pure mechanical grinding so toxic solvent is no longer needed. Furthermore, the dispersibility of TiO_2 nanoparticles in regenerated cellulose/solvent is poor, and phase separation between nanoparticles and cellulose occurs during film preparation. However, CNF is a nanofibrils rather than soluble molecules so the phase separation between TiO_2 particles and nanofibril network could be effectively prevented. However, the hydroxyl-richen cellulose shows strong hydrophilicity, which inevitably results in high electric leakage, high dielectric loss, low breakdown strength and low energy densities in humid environments (Shimizu et al. 2016; Yang et al. 2018a, b). Many studies have tended to focus on further improving the dielectric constant of cellulose nanopapers by introducing conductive fillers (Inui et al. 2015; Ji et al. 2017; Kafy et al. 2015b; Milovidova et al. 2014) but little attention has been paid on reducing dielectric loss.

Herein, we prepared a high dielectric composite film based on TiO_2 and CNF by a solution casting method. TiO_2 has a high dielectric constant (ε_r = 63.7 at 1 MHz), low dielectric loss ($\tan\delta < 0.051$) (Wypych et al. 2014) and is stable in a broad temperature range (< 1000 °C). Besides, the hydrophilic property of TiO_2 offers a way out for homogeneous mixing with CNF suspension. Thus, TiO_2 is a promising candidate for CNF based dielectrics. Homogenous composite films were made by mechanically mixing TiO_2 nanoparticles with CNF. The relative dielectric constant (ε_r) and dielectric loss ($\tan\delta$) were studied as the function of frequency and filler content. The effects of hot-press treatment on dielectric properties, microscopy, thermal stability, dynamic mechanical properties, and hydrophilicity of composite films were also studied.

Experimental

Materials

Both CNF slurry and 2,2,6,6-tetramethylpiperidinooxy (TEMPO)-oxidized CNF (TCNF) slurry were purchased from the University of Maine, with solid content of 3.4 wt% CNF and 1.1 wt% TCNF, respectively (Fukuzumi et al. 2010; Isogai et al. 2011; Kumar et al. 2014; Osong et al. 2016; Postek et al. 2013; Sacui et al. 2014; Saito et al. 2009; Stelte and Sanadi 2009). TiO_2 nanoparticles of diameter ~ 21 nm (P25) were purchased from Nippon Aerosil Co. Ltd.

Preparation of CNF/TiO_2 composite film

The purchased CNF and TCNF were diluted into 0.34 wt% and 0.30 wt% respectively by distilled water. According to the dry weight percentage, a certain amount of TiO_2 was added, then the solution was stirred homogeneously by a homogenizer for 10 min before poured into a petri dish. The dried film was obtained after being put in a fume for 2–4 days. After being hot-pressed under 80 °C and 1.1 MPa for 3 h, light yellow, flat and thin films were obtained. At least three samples were prepared for each composition. The thickness of the sample films was in the range of 30–100 μm. Figure 1 shows the flow diagram of the preparation of the CNF/TiO_2 composite film.

Characterizations

Morphologies of both surface and cross-section of the composite films were analyzed by thermally assisted field emission scanning electron microscope (TFE-SEM, LEO 1530, Germany) at an accelerating voltage of 10 kV. The composite films were sputtered with

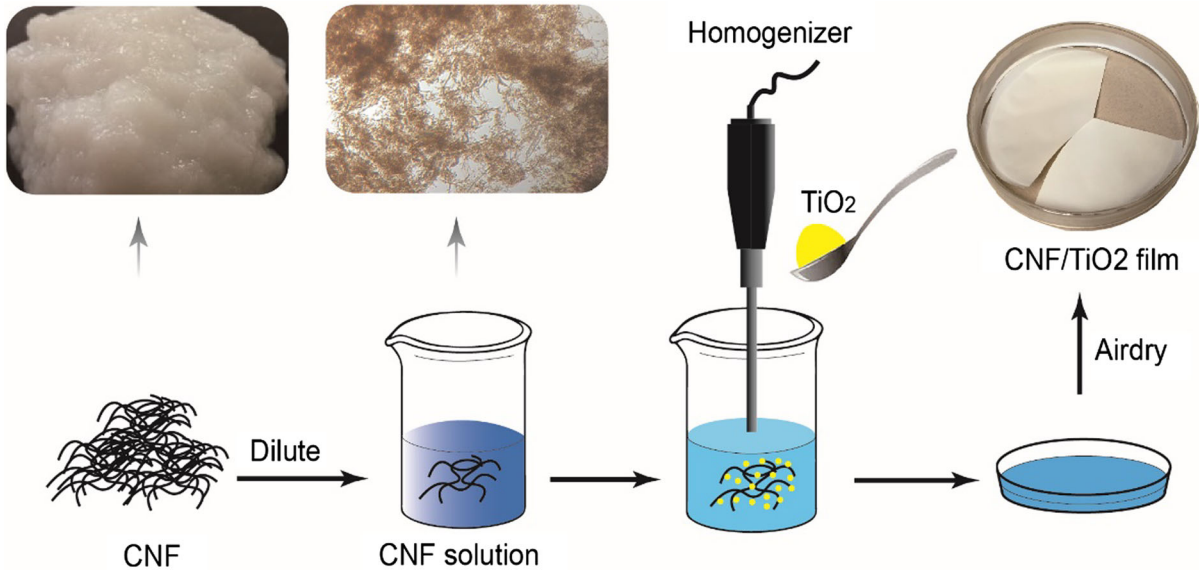

Fig. 1 The flow diagram illustrates the preparation of CNF/TiO_2 composite film

gold in vacuum to avoid accumulation of charge before observation.

Thermogravimetric analysis and differential scanning calorimetry (TGA–DTA) was performed on a simultaneous thermal analyzer (PerkinElmer STA6000, USA), ranging from 35 to 700 °C with a heating rate of 10 °C min^{-1} under nitrogen atmosphere and hold at 105 °C for 10 min before heading to a higher temperature.

The dielectric properties of sample films were measured by an LCR meter (Keysight E4980 with a 16451B fixture, USA) in the frequency range of 20 Hz–2 MHz. The test for each sample film was repeated at least five times. The thickness of the sample film was measured by a micrometer and was averaged over seven measurements on each sample. Unless otherwise stated, the dielectric constant of a material refers to the relative dielectric constant, which is the ratio of its absolute dielectric constant to the dielectric constant of vacuum. The relative dielectric constants (ε_r) of the sample films were calculated by Eq. (1)

$$C = \varepsilon_0 \varepsilon_r \frac{A}{d} \tag{1}$$

where C is the capacitance; ε_0 is the absolute dielectric constant of vacuum, $\varepsilon_0 = 8.854 \times 10^{-12}$ F/m; A is the electrode area, $A = 1.963 \times 10^{-12}$ m^2; d is the thickness of the sample film.

Tensile strength and ultimate elongation were studied with a dynamic mechanical analyzer DMA (Q800, TA Instruments, New Castle, DE, USA) with a test rate of 10% min^{-1} at room temperature. The film specimens were 5 mm wide and 20 mm long. At least four specimens were tested for each sample.

The densities of the sample films were calculated by Eq. (2)

$$d = \frac{m}{A \times t} \tag{2}$$

where d is the density, m is the weight, A is the surface area, and t is the thickness.

Results and discussion

Microscopy

Figure 2 shows the surface and cross-section morphologies of pure CNF and TiO_2 (50 wt%)/CNF composite film. The CNF was typically dozens of micrometers long with a diameter lower than 0.3 μm, and part of CNFs aggregated with each other (as shown in red circle). However, unlike normal paper which has a porous structure, no obvious pore was observed in pure CNF film. Figure 2b shows some level laminated structures with obvious layer gaps that might result from the peeling during the sample

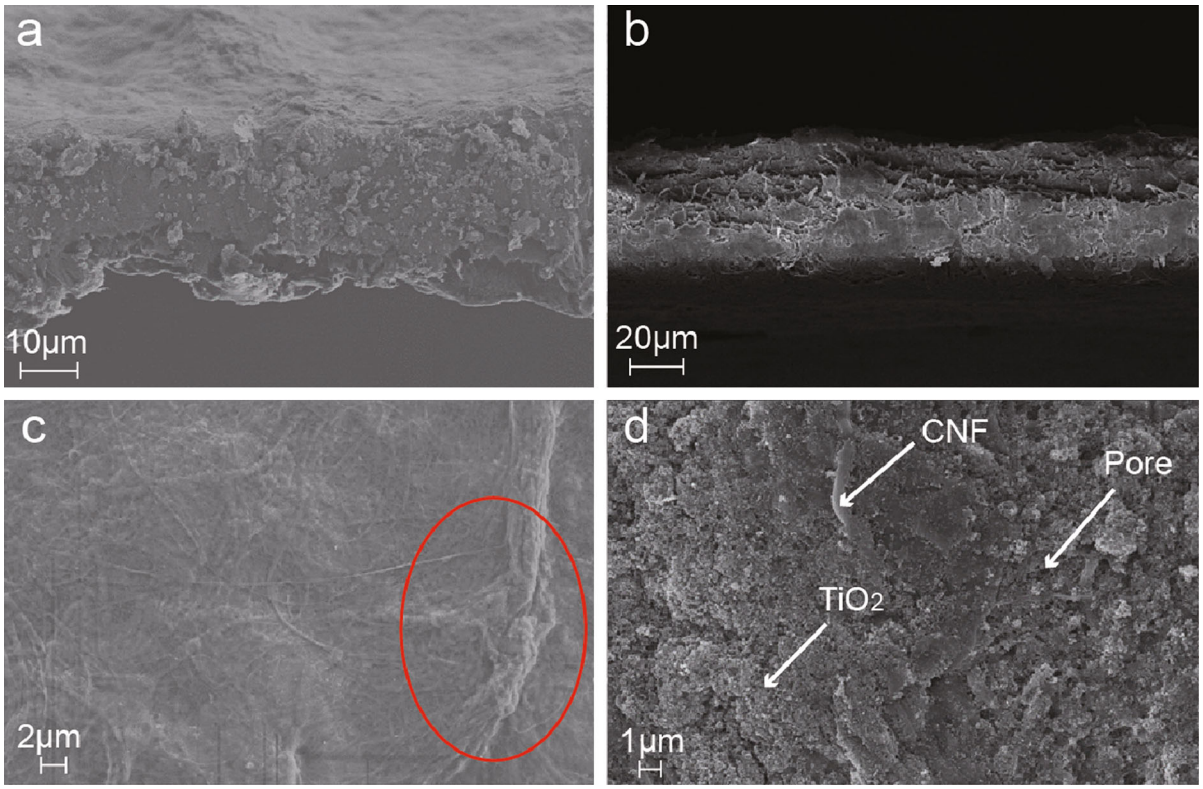

Fig. 2 Cross-section and surface SEM images of pure CNF (**a**, **c**) and hot-pressed CNF/TiO_2 (50 wt%) (**b**, **d**)

preparation. A dense layer and much smoother surface were observed, and it might result from the hot-press treatment. Figure 2d illustrates the distribution of TiO_2 in CNF. Because of the poor capability between the inorganic filler and organic matrix, there were some small pores, which had great influence on the properties of the composite film.

Dielectric properties

Prior to study the dielectric properties, a series of dielectric tests with different levels of oscillation signal (OSC level) was conducted. As shown in Fig. 3, the OSC level was adjusted in the range of 0.1–2 V. At lower OSC level of 0.1–1.5 V, the dielectric constant increased with the increase of OSC level, and the growth rate was decreased. After OSC level reached 2.0 V, the dielectric constant started to decrease. The same results were obtained in other composite films with different TiO_2 content. It illustrated that the testing electric field starts to overpass the breakdown strength of the films. Higher OSC level brings a higher

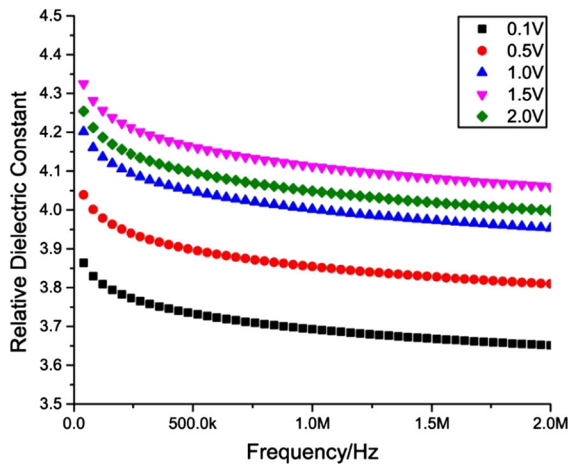

Fig. 3 The influence of OSC level on the dielectric test (50 wt% TiO_2/TCNF)

risk of breakdown. Thus, the following dielectric tests were conducted with OSC level at 1.0 V.

Figure 4 shows the influence of frequency and filler content on relative dielectric constant (ε_r) and dielectric loss (tan δ). With the increase of frequency, both ε_r

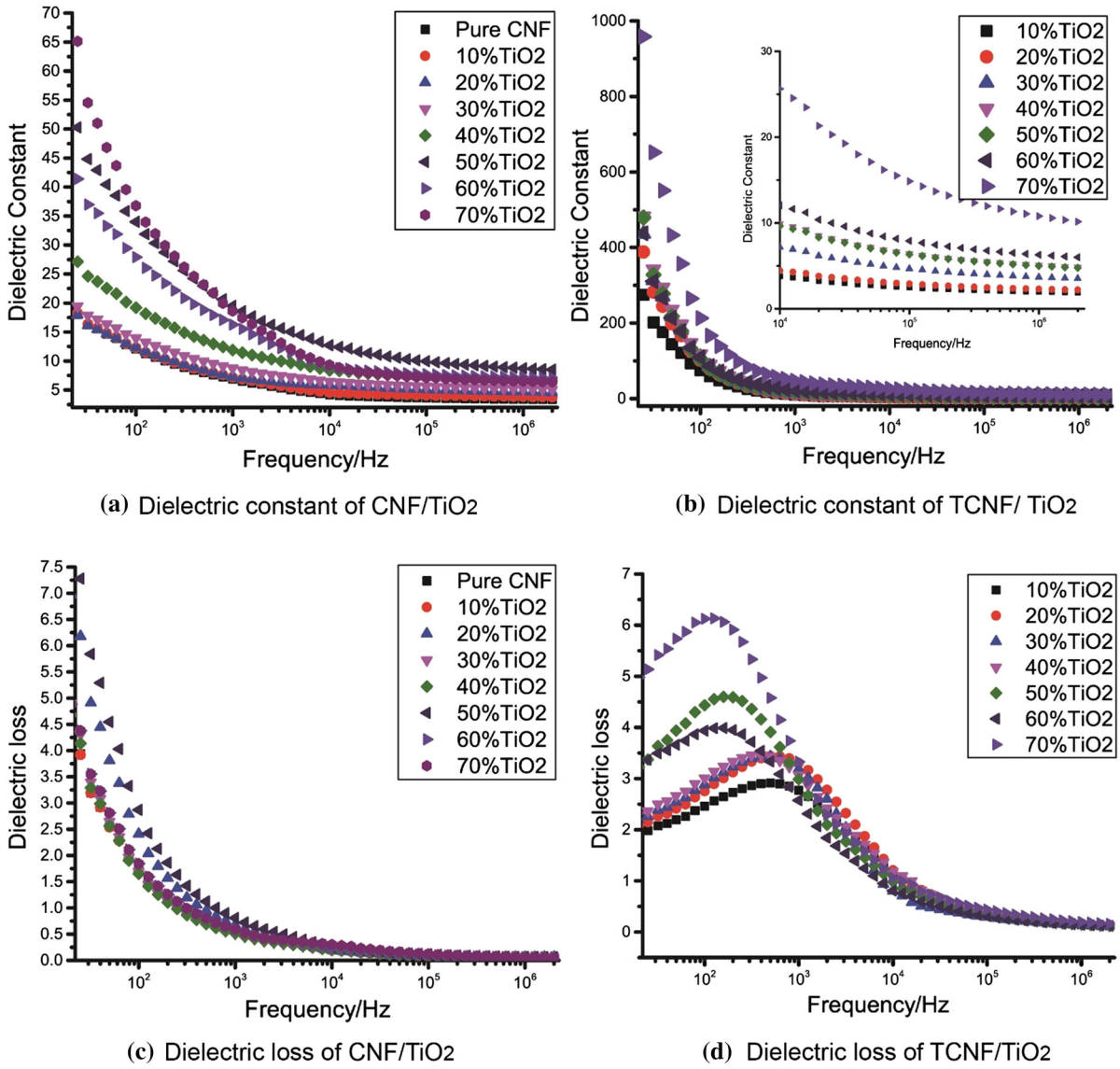

Fig. 4 The influence of frequency and filler content on the dielectric constant and dielectric loss

and tanδ decreased. In the lower range of 20–100 kHz, sharp reductions were observed. It was caused by the electrode polarization which took place at the interface between metal electrode and samples, and Maxwell–Wagner–Sillars interfacial polarization which can be observed at the interface between CNF and TiO_2 in inhomogeneous materials (Emmert et al. 2011; Lu and Zhang 2006; Samet et al. 2015; Anju and Narayanankutty 2016; Mohiuddin et al. 2015). Resulted from the interfacial polarization, the test results of ε_r and tanδ at the point of 20 Hz were abnormally high (several hundred or even higher) and were not showed in Fig. 4. In the higher frequency range of above 500 kHz, the reduction of both ε_r and tanδ tended to be flatter and showed much less dependence on frequency and filler content, which indicated that electronic and atomic polarization and orientation polarization started to play a predominant role.

The dielectric properties of the composite films can be explained by the multi-layered core model (Tanaka et al. 2005). According to this model, the interface of filler particle is chemically consisting of a bonded layer, a bound layer, a loose layer, and an electric double layer overlapping the above three layers. The

addition of nano-sized TiO_2 has contradicted effects on the dielectric properties. On the one hand, nano-sized TiO_2 introduced large surface areas for interfacial polarization compared with micro-sized TiO_2 (Kafy et al. 2015a), resulting in an extraordinary increase of both ε_r and tanδ in the low frequency range. On the other hand, the bonded layer and bound layer of the nanoparticles impair the motion of dipoles, leading to a reduction of ε_r and tanδ. And the dipoles and ionic carriers in the loose layer may act inversely. The far-field effect caused by the double electric layer makes the neighbored nano-particles collaborate with each other. The imperfection of heterogeneous structures can increase ε_r and tanδ. With the interfacial polarization becoming weak in the high frequency range, TiO_2 content showed less effect. In the case of micro-sized TiO_2, the increased ε_r is usually explained in term of the Lichtenecker–Rother logarithmic law of mixing (Tanaka 2005).

The ε_r of CNF/TiO_2 increased with the increasing of TiO_2 content in the range of 0–50 wt%. The maximum dielectric constant was 19.51 (at 1 kHz) at 50 wt%. As the TiO_2 content continued to increase, the dielectric constant decreased. It was caused by the aggregation of TiO_2 and the appearance of pores, as shown in SEM images. In the range of 0–70 wt%, the dielectric loss showed less dependency on TiO_2 content and fluctuated in the range of 0.51–0.81 (at 1 kHz). The ε_r of TCNF/TiO_2 increased with TiO_2 content in the range of 10–70 wt% and reached the maximum value of 47.15 (at 1 kHz) at 70 wt%. The dielectric loss of TCNF/TiO_2 composite films also showed less dependency on TiO_2 content and was fluctuated in the range of 2.57–3.32 (at 1 kHz). Generally, the dielectric loss of TCNF/TiO_2 composite films was three times higher than CNF/TiO_2 composite films, which was caused by the residual ions after TEMPO oxidation treatment of CNF. Thus, from the perspective of reliability and energy saving, CNF/TiO_2 was better than TCNF/TiO_2. Compared with other reported CNF based dielectrics, our CNF/TiO_2 showed a much lower dielectric loss.

Thermal properties

In order to study the thermal stability of the composite films, TGA–DTA measurements were conducted on a series of CNF/TiO_2 composite films with the TiO_2 content in the range of 10–50 wt%. Figure 5a, b shows the typical TGA–DTA curves for pure CNF and CNF/TiO_2 (50 wt%) composite film after hot-press treatment, respectively. In the low temperature region below 105 °C, weight losses of 5.66–2.95% on the TGA curve and an endothermic peak at 41 °C on the DTA curve were observed. It was caused by water evaporation (Chenampulli et al. 2019; Hassan et al. 2019; Jayaramudu et al. 2018a; Lizundia et al. 2016; Poyraz 2018; Poyraz et al. 2017a; Raghunathan et al. 2017; Zeng et al. 2016). The temperature was held at 105 °C for 10 min, and it was showed obviously on the DTA curve as a marked drop. The 5% decomposition temperature of the sample films was 291–302 °C, which indicated that the TiO_2/CNF has a low water absorption and good thermostability. The fluctuation of the DTA curve and sharply loss of weight around 400 °C showed the decomposition of CNF. At 700 °C, for the composite films, the residual weight percentage of sample films was per the TiO_2 content, which indicated that CNF had been completely decomposed at this temperature. However, for pure CNF, the weight percentage was 15%. It indicated that the addition of TiO_2 accelerates the thermal degradation of CNF.

Dynamic mechanical property

Figure 5c shows the DMA test results of CNF/TiO_2 composite films. All the stress–strain curves show "S" shape, suggesting that with the increase of strain, the stress first increased slowly, then sharply, and turned to be slow again, and finally the sample broke down, which is a typical property of flexible films. For pure CNF, hot-pressing treatment improved the strain at break from 7.65 to 10.92% with the stress slightly decreased from 76.91 to 76.59 MPa, which was resulted from better bounding between CNFs after hot-pressing treatment. However, CNF/TiO_2 (50 wt%) composite film has a contract result. After hot-pressing, the strain at break decreased from 5.45 to 2.63%, and the stress increased from 12.68 to 17.71 MPa, which may be caused by the weak bonding between TiO_2 particles and CNFs.

Density

Figure 5d shows the densities of untreated and hot-pressed (HP) CNF films. Pure CNF films have higher densities than CNF/TiO_2 (50 wt%) although the

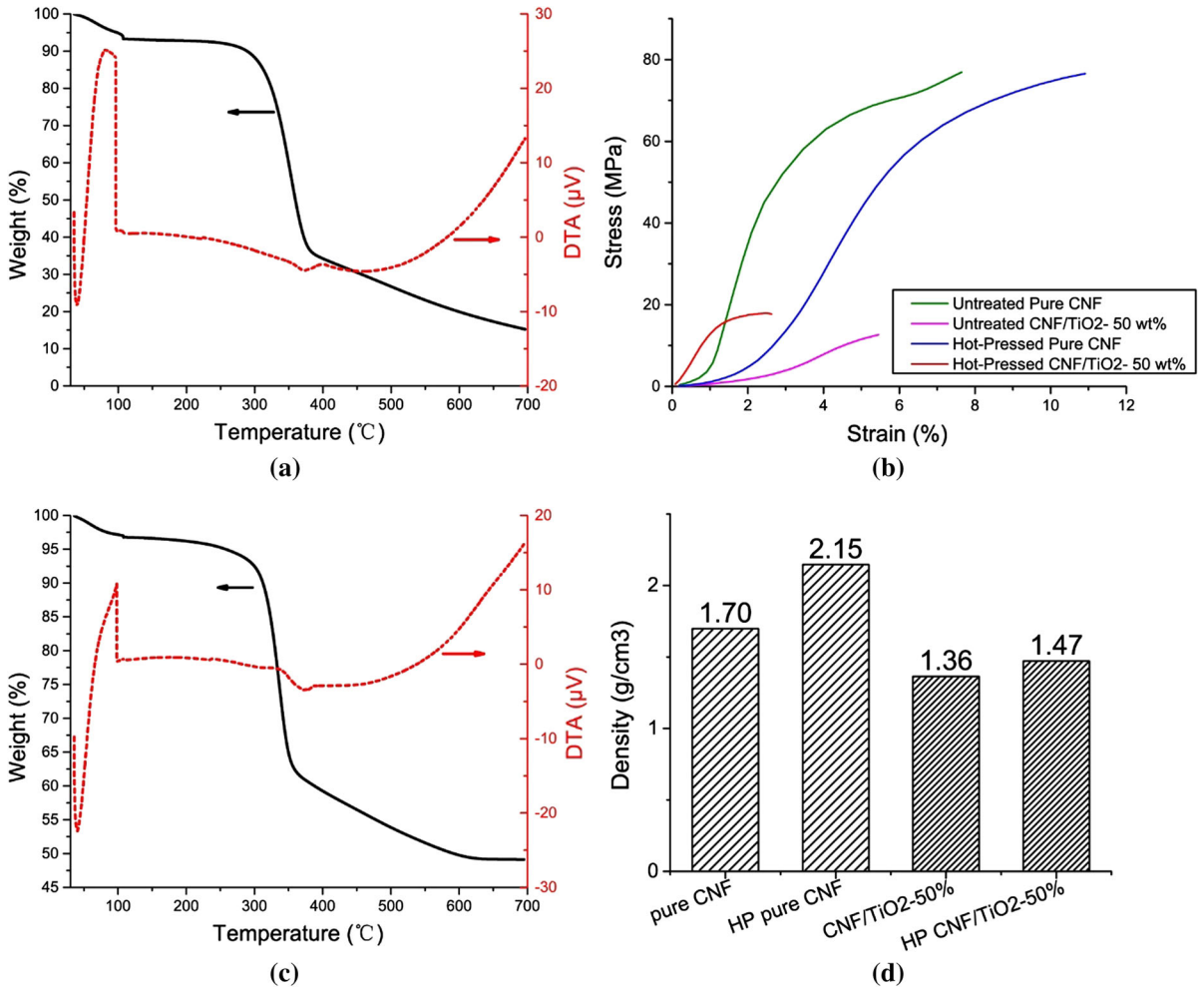

Fig. 5 **a** TGA–DTA curves of pure CNF film. **b** TGA–DTA curves of CNF/TiO_2 (50 wt%) composite film after hot-press treatment. **c** Dynamic mechanical properties of hot-pressed (HP) and untreated CNF/TiO_2 composite films with different TiO_2 content. **d** Densities of untreated and hot-pressed (HP) CNF films

density of TiO_2 is much higher than cellulose. Because the poor bonding between CNF and TiO_2, a looser structure of the films was obtained by adding TiO_2 particles, which is confirmed by SEM images shown in Fig. 2. Hot-pressing could improve the density of CNF films, and the rise of pure CNF is much higher than that of CNF/TiO_2 (50 wt%), suggesting that the pores in the CNF/TiO_2 films are hardly be removed by physical treatment.

Conclusions

In conclusion, a high dielectric film was prepared under facile condition. The relative dielectric constant of CNF/TiO_2 composite film reached 19.51 (at 1 kHz). Compared with pure CNF films (ε_r = 6.92 at 1 kHz), the ε_r of composite films was improved about three times. It was also illustrated that hot-pressed CNF/TiO_2 had good flexibility and thermal stability. The addition of TiO_2 particles reduces the cellulose–cellulose bonding so generates more pores in the films, which has significant impacts on both dielectric and physical strength properties.

References

Abdel-karim AM, Salama AH, Hassan ML (2018) Electrical conductivity and dielectric properties of nanofibrillated cellulose thin films from bagasse. J Phys Org Chem 31(9):e3851. https://doi.org/10.1002/poc.3851

Al-Saygh A, Ponnamma D, AlMaadeed M, Vijayan P, Karim A, Hassan M (2017) Flexible pressure sensor based on PVDF nanocomposites containing reduced graphene oxide–titania hybrid nanolayers. Polymers 9(2):33. https://doi.org/10.3390/polym9020033

Alam MM, Ghosh SK, Sarkar D, Sen S, Mandal D (2017) Improved dielectric constant and breakdown strength of gamma-phase dominant super toughened polyvinylidene fluoride/TiO_2 nanocomposite film: an excellent material for energy storage applications and piezoelectric throughput. Nanotechnology 28(1):015503. https://doi.org/10.1088/0957-4484/28/1/015503

Anju V, Narayanankutty SK (2016) Polyaniline coated cellulose fiber/polyvinyl alcohol composites with high dielectric permittivity and low percolation threshold. AIP Adv 6(1):015109

Bonardd S, Robles E, Barandiaran I, Saldias C, Leiva A, Kortaberria G (2018) Biocomposites with increased dielectric constant based on Chitosan and nitrile-modified cellulose nanocrystals. Carbohydr Polym 199:20–30. https://doi.org/10.1016/j.carbpol.2018.06.088

Chang CJ, Tsai MH, Chen GS, Wu MS, Hung TW (2009) Preparation and properties of porous polyimide films with TiO_2/polymer double shell hollow spheres. Thin Solid Films 517(17):4966–4969. https://doi.org/10.1016/j.tsf.2009.03.201

Chenampulli S, Unnikrishnan G, Thomas S, Narine SS (2019) Novel ethylene diamine functionalised nanocellulose/poly(ethylene-co-acrylic acid) composites for biomedical applications. Cellulose 26(3):1795–1809. https://doi.org/10.1007/s10570-018-02227-6

Chiang C, Popielarz R (2002) Polymer composites with high dielectric constant. Ferroelectrics 275(1):1–9

Dang Z-M (2018) 1—Introduction. In: Dang Z-M (ed) Dielectric polymer materials for high-density energy storage. William Andrew Publishing, Oxford, pp 1–9. https://doi.org/10.1016/B978-0-12-813215-9.00001-4

Deshmukh K, Ahamed MB, Deshmukh RR, Pasha SKK, Sadasivuni KK, Ponnamma D, AlMaadeed MA (2017) Striking multiple synergies in novel three-phase fluoropolymer nanocomposites by combining titanium dioxide and graphene oxide as hybrid fillers. J Mater Sci: Mater Electron 28(1):559–575. https://doi.org/10.1007/s10854-016-5559-1

Dou Z, Liu W, Lin T, Zhou K, Hang L (2017) High performance capacitors via aligned TiO_2 nanowire array. Appl Phys Lett. https://doi.org/10.1063/1.4979407

Du X, Zhang Z, Liu W, Deng Y (2017) Nanocellulose-based conductive materials and their emerging applications in energy devices—a review. Nano Energy 35:299–320. https://doi.org/10.1016/j.nanoen.2017.04.001

Emmert S, Wolf M, Gulich R, Krohns S, Kastner S, Lunkenheimer P, Loidl A (2011) Electrode polarization effects in broadband dielectric spectroscopy. Eur Phys J B 83(2):157–165. https://doi.org/10.1140/epjb/e2011-20439-8

Feng Y, Yin JH, Chen MH, Song MX, Su B, Lei QQ (2013) Effect of nano-TiO_2 on the polarization process of polyimide/TiO_2 composites. Mater Lett 96:113–116. https://doi.org/10.1016/j.matlet.2013.01.037

Feng Y, Yin JH, Chen MH, Liu XX, Su B, Fei WD, Lei QQ (2014) Influence of interface on the electrical properties of polyimide/TiO_2 composite films. IEEE Trans Dielectr Electr Insul 21(4):1501–1508. https://doi.org/10.1109/Tdei.2014.004322

Fujisaki Y et al (2014) Transparent nanopaper-based flexible organic thin-film transistor array. Adv Funct Mater 24(12):1657–1663. https://doi.org/10.1002/adfm.201303024

Fukuzumi H, Saito T, Okita Y, Isogai A (2010) Thermal stabilization of TEMPO-oxidized cellulose. Polym Degrad Stab 95(9):1502–1508. https://doi.org/10.1016/j.polymdegradstab.2010.06.015

Gan WC, Abd Majid WH (2014) Effect of TiO_2 on enhanced pyroelectric activity of PVDF composite. Smart Mater Struct. https://doi.org/10.1088/0964-1726/23/4/045026

Gaspar D et al (2014) Nanocrystalline cellulose applied simultaneously as the gate dielectric and the substrate in flexible field effect transistors. Nanotechnology 25(9):094008. https://doi.org/10.1088/0957-4484/25/9/094008

Hassan ML, Ali AF, Salama AH, Abdel-Karim AM (2019) Novel cellulose nanofibers/barium titanate nanoparticles nanocomposites and their electrical properties. J Phys Org Chem 32(2):e3897

Inui T, Koga H, Nogi M, Komoda N, Suganuma K (2014) High-dielectric paper composite consisting of cellulose nanofiber and silver nanowire. In: 14th IEEE international conference on nanotechnology, pp 470–473

Inui T, Koga H, Nogi M, Komoda N, Suganuma K (2015) A miniaturized flexible antenna printed on a high dielectric constant nanopaper composite. Adv Mater 27(6):1112–1116. https://doi.org/10.1002/adma.201404555

Ishmael SA et al (2014) Thermal conductivity and dielectric properties of a TiO_2-based electrical insulator for use with high temperature superconductor-based magnets. Supercond Sci Technol 27(9):9. https://doi.org/10.1088/0953-2048/27/9/095018

Isogai A, Saito T, Fukuzumi H (2011) TEMPO-oxidized cellulose nanofibers. Nanoscale 3(1):71–85. https://doi.org/10.1039/c0nr00583e

Jayaramudu T, Ko H-U, Kim H, Kim J, Muthoka R, Kim J (2018a) Electroactive hydrogels made with polyvinyl alcohol/cellulose nanocrystals. Materials 11(9):1615

Jayaramudu T, Ko HU, Kim HC, Kim JW, Muthoka RM, Kim J (2018b) Electroactive hydrogels made with polyvinyl alcohol/cellulose nanocrystals. Materials 11(9):11. https://doi.org/10.3390/ma11091615

Ji S et al (2017) High dielectric performances of flexible and transparent cellulose hybrid films controlled by multidimensional metal nanostructures. Adv Mater 29(24):1700538. https://doi.org/10.1002/adma.201700538

Kafy A, Sadasivuni KK, Akther A, Min S-K, Kim J (2015a) Cellulose/graphene nanocomposite as multifunctional electronic and solvent sensor material. Mater Lett 159:20–23

Kafy A, Sadasivuni KK, Kim HC, Akther A, Kim J (2015b) Designing flexible energy and memory storage materials using cellulose modified graphene oxide nanocomposites. Phys Chem Chem Phys 17(8):5923–5931. https://doi.org/10.1039/c4cp05921b

Kizilkaya C, Dumludag F, Karatas S, Apohan NK, Altindal A, Gungor A (2012) The effect of titania content on the physical properties of polyimide/titania nanohybrid films. J Appl Polym Sci 125(5):3802–3810. https://doi.org/10.1002/app.35292

Koytepe S, Seckin T, Kivrilcim N, Adiguzel HI (2008) Synthesis and dielectric properties of polyimide–titania hybrid composites. J Inorg Organomet Polym Mater 18(2):222–228. https://doi.org/10.1007/s10904-007-9169-5

Kumar V et al (2014) Comparison of nano- and microfibrillated cellulose films. Cellulose 21(5):3443–3456. https://doi.org/10.1007/s10570-014-0357-5

Kumari A, Ghosh BD (2018) La doped barium titanate/polyimide nanocomposites: a study of the effect of La doping and investigation on thermal, mechanical and high dielectric properties. J Appl Polym Sci 135(47):12. https://doi.org/10.1002/app.46826

Lay M, Meng S, Ramli MR, Ahmad Z, Ismail H, Huat TS, Todo M (2018) Interphase volume calculation of polyimide/TiO_2 nanofibers nanocomposite based on dielectric constant model and its effect on glass transition. J Mater Sci: Mater Electron 29(24):20742–20749. https://doi.org/10.1007/s10854-018-0215-6

Le Bras D, Stromme M, Mihranyan A (2015) Characterization of dielectric properties of nanocellulose from wood and algae for electrical insulator applications. J Phys Chem B 119(18):5911–5917. https://doi.org/10.1021/acs.jpcb.5b00715

Lee WH, Wang CC (2010) Effect of nanocomposite gate-dielectric properties on pentacene microstructure and field-effect transistor characteristics. J Nanosci Nanotechnol 10(2):762–769. https://doi.org/10.1166/jnn.2010.1817

Lee WH, Wang CC, Ho JC (2009) Improved performance of pentacene field-effect transistors using a nanocomposite gate dielectric. J Vac Sci Technol, B 27(2):601–605. https://doi.org/10.1116/1.3093881

Lee WH, Liu CT, Lee YC (2012) Study on preparation of high-k organic-inorganic thin film for organic-inorganic thin film transistor gate dielectric application. Jpn J Appl Phys 51(6):7. https://doi.org/10.1143/jjap.51.061603

Lin JQ, Wang Y, Yang WL, Lu HW (2017) Balance of mechanical and electrical performance in polyimide/nano titanium dioxide prepared by an in-sol method. J Appl Polym Sci 134(13):9. https://doi.org/10.1002/App.44666

Lizundia E et al (2016) Cu-coated cellulose nanopaper for green and low-cost electronics. Cellulose 23(3):1997–2010

Lu HB, Zhang XY (2006) Influence of the relaxation of Maxwell–Wagner–Sillars polarization and dc conductivity on the dielectric behaviors of nylon 1010. J Appl Phys 100(5):054104. https://doi.org/10.1063/1.2336494

Lu HW, Lin JQ, Yang WL, Liu LZ, Wang Y, Chen GR, Huang W (2017) Effect of nano-TiO_2 surface modification on polarization characteristics and corona aging performance of polyimide nano-composites. J Appl Polym Sci 134(29):9. https://doi.org/10.1002/app.45101

Madusanka N, Shivareddy SG, Hiralal P, Eddleston MD, Choi Y, Oliver RA, Amaratunga GA (2016) Nanocomposites of TiO_2/cyanoethylated cellulose with ultra high dielectric constants. Nanotechnology 27(19):195402

Madusanka N, Shivareddy SG, Eddleston MD, Hiralal P, Oliver RA, Amaratunga GA (2017) Dielectric behaviour of montmorillonite/cyanoethylated cellulose nanocomposites. Carbohydr Polym 172:315–321

Meena JS et al (2012) Facile synthetic route to implement a fully bendable organic metal–insulator–semiconductor device on polyimide sheet. Org Electron 13(5):721–732. https://doi.org/10.1016/j.orgel.2012.01.007

Milinskii AY, Baryshnikov SV, Thuong NH (2018) Dielectric properties of nanocomposites based on potassium iodate with porous nanocrystalline cellulose. Ferroelectrics 524(1):181–188. https://doi.org/10.1080/00150193.2018.1432830

Milovidova SD, Rogazinskaya OV, Sidorkin AS, Thuong NH, Grohotova EV, Popravko NG (2014) Dielectric properties of composites based on nanocrystalline cellulose and triglycine sulfate. Ferroelectrics 469(1):116–119. https://doi.org/10.1080/00150193.2014.949132

Mohiuddin M, Sadasivuni KK, Mun S, Kim J (2015) Flexible cellulose acetate/graphene blueprints for vibrotactile actuator. RSC Adv 5(43):34432–34438

Novac OC, Maries GRE, Chira D, Novac M (2017) Study concerning the influence of the grinding percentage on some electrical properties of PA 6.6, POM and ABS by methods for determining relative permittivity and the dielectric dissipation factor. Mater Plast 54(3):453–460

Olariu MA, Hamciuc C, Okrasa L, Hamciuc E, Dimitrov L, Kalvachev Y (2017) Electrical properties of polyimide composite films containing TiO_2 Nanotubes. Polym Compos 38(11):2584–2593. https://doi.org/10.1002/pc.23851

Osong SH, Norgren S, Engstrand P (2016) Processing of wood-based microfibrillated cellulose and nanofibrillated cellulose, and applications relating to papermaking: a review. Cellulose 23(1):93–123. https://doi.org/10.1007/s10570-015-0798-5

Paniagua SA, Kim Y, Henry K, Kumar R, Perry JW, Marder SR (2014) Surface-initiated polymerization from barium titanate nanoparticles for hybrid dielectric capacitors. ACS Appl Mater Interfaces 6(5):3477–3482. https://doi.org/10.1021/am4056276

Park HH, Choi Y, Park DJ, Cho SY, Yun YS, Jin HJ (2013) Enhanced dielectric properties of electrospun titanium dioxide/polyvinylidene fluoride nanofibrous composites. Fibers Polym 14(9):1521–1525. https://doi.org/10.1007/s12221-013-1521-5

Postek MT, Moon RJ, Rudie AW, Bilodeau MA (2013) Production and applications of cellulose. Tappi Press, Peachtree Corners

Poyraz B (2018) Enzyme treated CNF biofilms: characterization. Int J Biol Macromol 117:713–720. https://doi.org/10.1016/j.ijbiomac.2018.05.222

Poyraz B, Tozluoğlu A, Candan Z, Demir A (2017a) Matrix impact on the mechanical, thermal and electrical properties of microfluidized nanofibrillated cellulose composites. J Polym Eng 37(9):921–931. https://doi.org/10.1515/polyeng-2017-0022

Poyraz B, Tozluoglu A, Candan Z, Demir A, Yavuz M (2017b) Influence of PVA and silica on chemical, thermo-mechanical and electrical properties of Celluclast-treated nanofibrillated cellulose composites. Int J Biol Macromol 104(Pt A):384–392. https://doi.org/10.1016/j.ijbiomac.2017.06.018

Prabakaran K, Mohanty S, Nayak SK (2014) Influence of surface modified TiO_2 nanoparticles on dielectric properties of PVdF–HFP nanocomposites. J Mater Sci: Mater Electron 25(10):4590–4602. https://doi.org/10.1007/s10854-014-2209-3

Qi FW, Chen N, Wang Q (2017) Preparation of PA11/$BaTiO_3$ nanocomposite powders with improved processability, dielectric and piezoelectric properties for use in selective laser sintering. Mater Design 131:135–143. https://doi.org/10.1016/j.matdes.2017.06.012

Qi FW, Chen N, Wang Q (2018) Dielectric and piezoelectric properties in selective laser sintered polyamide11/$BaTiO_3$/CNT ternary nanocomposites. Mater Design 143:72–80. https://doi.org/10.1016/j.matdes.2018.01.050

Raghunathan SP, Narayanan S, Poulose AC, Joseph R (2017) Flexible regenerated cellulose/polypyrrole composite films with enhanced dielectric properties. Carbohydr Polym 157:1024–1032

Rajala S et al (2016) Cellulose nanofibril film as a piezoelectric sensor material. ACS Appl Mater Interfaces 8(24):15607–15614. https://doi.org/10.1021/acsami.6b03597

Rekik H, Ghallabi Z, Royaud I, Arous M, Seytre G, Boiteux G, Kallel A (2013) Dielectric relaxation behaviour in semi-crystalline polyvinylidene fluoride (PVDF)/TiO_2 nanocomposites. Compos Part B Eng 45(1):1199–1206. https://doi.org/10.1016/j.compositesb.2012.08.002

Ribeiro C et al (2018) Electroactive poly(vinylidene fluoride)-based structures for advanced applications. Nat Protoc 13(4):681–704. https://doi.org/10.1038/nprot.2017.157

Sacui IA et al (2014) Comparison of the properties of cellulose nanocrystals and cellulose nanofibrils isolated from bacteria, tunicate, and wood processed using acid, enzymatic, mechanical, and oxidative methods. ACS Appl Mater Interfaces 6(9):6127–6138. https://doi.org/10.1021/am500359f

Saito T, Hirota M, Tamura N, Kimura S, Fukuzumi H, Heux L, Isogai A (2009) Individualization of nano-sized plant cellulose fibrils by direct surface carboxylation using tempo catalyst under neutral conditions. Biomacromolecules 10(7):1992–1996. https://doi.org/10.1021/bm900414t

Samet M, Levchenko V, Boiteux G, Seytre G, Kallel A, Serghei A (2015) Electrode polarization vs. Maxwell–Wagner–Sillars interfacial polarization in dielectric spectra of materials: characteristic frequencies and scaling laws. J Chem Phys 142(19):194703. https://doi.org/10.1063/1.4919877

Shi L et al (2018) Dielectric gels with ultra-high dielectric constant, low elastic modulus, and excellent transparency. NPG Asia Mater 10(8):821

Shimizu M, Saito T, Isogai A (2016) Water-resistant and high oxygen-barrier nanocellulose films with interfibrillar cross-linkages formed through multivalent metal ions. J Membr Sci 500:1–7. https://doi.org/10.1016/j.memsci.2015.11.002

Stelte W, Sanadi AR (2009) Preparation and characterization of cellulose nanofibers from two commercial hardwood and softwood pulps. Ind Eng Chem Res 48(24):11211–11219. https://doi.org/10.1021/ie9011672

Su R et al (2016) High energy density performance of polymer nanocomposites induced by designed formation of $BaTiO_3$@sheet-IikeTiO$_2$ hybrid nanofillers. J Phys Chem C 120(22):11769–11776. https://doi.org/10.1021/acs.jpcc.6b01853

Tanaka T (2005) Dielectric nanocomposites with insulating properties. IEEE Trans Dielectr Electr Insul 12(5):914–928. https://doi.org/10.1109/TDEI.2005.1522186

Tanaka T, Kozako M, Fuse N, Ohki Y (2005) Proposal of a multi-core model for polymer nanocomposite dielectrics. IEEE Trans Dielectr Electr Insul 12(4):669–681. https://doi.org/10.1109/TDEI.2005.1511092

Tang R, Liggat JJ, Siew WH (2018) Filler and additive effects on partial discharge degradation of PET films used in PV devices. Polym Degrad Stab 150:148–157. https://doi.org/10.1016/j.polymdegradstab.2018.02.003

Thomas S, Deepu VN, Mohanan P, Sebastian MT (2008) Effect of filler content on the dielectric properties of PTFE/$ZnAl_2O_4$-TiO_2 composites. J Am Ceram Soc 91(6):1971–1975. https://doi.org/10.1111/j.1551-2916.2008.02365.x

Topala I, Dumitrascu N, Pohoata V (2007) Influence of plasma treatments on the hemocompatibility of PET and PET + TiO_2 films. Plasma Chem Plasma Process 27(1):95–112. https://doi.org/10.1007/s11090-006-9046-y

Wang D, Dang Z-M (2018) Processing of polymeric dielectrics for high energy density capacitors. In: Dielectric polymer materials for high-density energy storage. Elsevier, Amsterdam, pp 429-446

Wang SF, Wang YR, Cheng KC, Chen SH (2010a) Physical and electrical properties of polyimide/ceramic hybrid films prepared via non-hydrolytic sol–gel process. J Mater Sci: Mater Electron 21(1):104–110. https://doi.org/10.1007/s10854-009-9876-5

Wang Y, Zhou X, Chen Q, Chu BJ, Zhang QM (2010b) Recent development of high energy density polymers for dielectric capacitors. IEEE Trans Dielectr Electr Insul 17(4):1036–1042. https://doi.org/10.1109/Tdei.2010.5539672

Wang JC, Long YC, Sun Y, Zhang XQ, Yang H, Lin BP (2018) Fabrication and enhanced dielectric properties of polyimide matrix composites with core-shell structured $CaCu_3Ti_4O_{12}$@TiO_2 nanofibers. J Mater Sci: Mater Electron 29(9):7842–7850. https://doi.org/10.1007/s10854-018-8783-z

Wu GL, Li JL, Wang KK, Wang YQ, Pan C, Feng AL (2017) In situ synthesis and preparation of TiO_2/polyimide composite containing phenolphthalein functional group. J Mater Sci: Mater Electron 28(9):6544–6551. https://doi.org/10.1007/s10854-017-6343-6

Wypych A et al (2014) dielectric properties and characterisation of titanium dioxide obtained by different chemistry methods. J Nanomater. https://doi.org/10.1155/2014/124814

Yagyu H, Ifuku S, Nogi M (2017) Acetylation of optically transparent cellulose nanopaper for high thermal and moisture resistance in a flexible device substrate. Flex Print Electron 2(1):7. https://doi.org/10.1088/2058-8585/aa60f4

Yang L, Ji HL, Zhu KJ, Wang J, Qiu JH (2016) Dramatically improved piezoelectric properties of poly(vinylidene fluoride) composites by incorporating aligned TiO_2@-MWCNTs. Compos Sci Technol 123:259–267. https://doi.org/10.1016/j.compscitech.2015.11.032

Yang J, Xie H, Chen H, Shi Z, Wu T, Yang Q, Xiong C (2018a) Cellulose nanofibril/boron nitride nanosheet composites with enhanced energy density and thermal stability by interfibrillar cross-linking through Ca 2+. J Mater Chem A 6(4):1403–1411. https://doi.org/10.1039/C7TA08188J

Yang Q, Zhang C, Shi Z, Wang J, Xiong C, Saito T, Isogai A (2018b) Luminescent and transparent nanocellulose films containing europium carboxylate groups as flexible dielectric materials. ACS Appl Nano Mater 1(9):4972–4979. https://doi.org/10.1021/acsanm.8b01112

Yin J et al (2014) Effect of MMT content on structure of polyimide/(TiO_2 + MMT) nanocomposite films. In: 2014 9th international forum on strategic technology (IFOST), pp 475–478. https://doi.org/10.1109/IFOST.2014.6991167

Yuan Y, Cui YR, Wu KT, Huang QQ, Zhang SR (2014) TiO_2 and SiO_2 filled PTFE composites for microwave substrate applications. J Polym Res 21(2):6. https://doi.org/10.1007/s10965-014-0366-y

Yuan Y, Wang J, Yao MH, Tang B, Li EZ, Zhang SR (2018) Influence of SiO_2 addition on properties of PTFE/TiO_2 microwave composites. J Electron Mater 47(1):633–640. https://doi.org/10.1007/s11664-017-5826-9

Zeng XL, Deng LB, Yao YM, Sun R, Xu JB, Wong CP (2016) Flexible dielectric papers based on biodegradable cellulose nanofibers and carbon nanotubes for dielectric energy storage. J Mater Chem C 4(25):6037–6044. https://doi.org/10.1039/c6tc01501h

Zha JW, Dang ZM, Song HT, Yin Y, Chen G (2010a) Dielectric properties and effect of electrical aging on space charge accumulation in polyimide/TiO_2 nanocomposite films. J Appl Phys 108(9):6. https://doi.org/10.1063/1.3506715

Zha JW, Dang ZM, Zhou T, Song HT, Chen G (2010b) Electrical properties of TiO_2-filled polyimide nanocomposite films prepared via an in situ polymerization process. Synth Metals 160(23–24):2670–2674. https://doi.org/10.1016/j.synthmet.2010.10.024

Zhou Y, Huang X, Huang J, Zhang L, Zhou Z (2018) Predicting the dielectric properties of nanocellulose-modified press-paper based on the multivariate analysis method. Molecules 23(7):1507. https://doi.org/10.3390/molecules23071507

Publisher's Note Springer Nature remains neutral with regard to jurisdictional claims in published maps and institutional affiliations.